JMEPEG (2011) 20:31–39
DOI: 10.1007/s11665-010-9661-x

1059-9495/$19.00

Path-Weighted Diffusivity Functions for Parameterization of Heat Deposition Processes

S.G. Lambrakos and K.P. Cooper

(Submitted March 11, 2010)

General parameterizations are constructed for spatial modulation of heat diffusion patterns according to energy deposition characteristics occurring within a volume of material where there exist inhomogeneous or anisotropic thermal diffusivity. These parameterizations are formulated in terms of path-weighted diffusivity functions. The construction of a general parameterization of energy deposition processes where spatially dependent thermal diffusivity exists is necessary for their inverse analysis. The structure of such a parameterization follows from the concepts of model and data spaces that imply the existence of an optimal parametric representation for a given class of inverse problems. Accordingly, the optimal parametric representation is determined by the characteristics of the available data, which, in principle, can contain both experimental measurements and numerical simulation data. Parameterizations for spatial modulation of heat diffusion follow from the observation that many different types of energy deposition processes can be represented by weighted sums of basis functions whose general forms are that of spatially modulated diffusion. The parameterizations presented are constructed according to a specific definition of the inverse heat deposition problem that provides a rigorous foundation for a highly flexible and general parameterization of energy deposition processes, which is essential for their inverse analysis.

Keywords fabricated metal, joining, modeling processes

1. Introduction

The general parameterization of heat deposition systems follows from the concept of a model space that establishes the existence of an optimal parametric representation for a given class of inverse problems (Ref 1). This property is related to the fact that inverse analyses based entirely on mathematical formulations representing physical theories are not generally well disposed in that these formulations are inherently based on direct-problem paradigms. In particular, the concept of a model space implies the existence of an optimal parametric representation for inverse analysis, which is not based on the existence of a complete set of representative physical theories, but rather on the characteristics, relative sizes, and completeness of data sets associated with or in practice available for that system, i.e., the data space. The parameterizations presented in this study are constructed according to the following concepts, which have been discussed previously. These concepts are the use of generalized functions, parameterizations using basis functions, general trend characteristics of energy deposition, energy source functions, and parameterizations for heat diffusion pattern modulation and filtering. In this article, we present the general parameterizations for spatial modulation of heat diffusion patterns according to energy deposition characteristics occurring within a volume of material where inhomogeneous or anisotropic thermal diffusivity exists. These parameterizations are formulated in terms of path-weighted diffusivity functions.

The organization of the subject areas presented here are as follows. First, a precise mathematical statement of the inverse problem to which the analysis methodology is to be applied is given. In that the range of inverse problems is vast, it is essential, even within the context of inverse heat transfer, to define precisely the inverse problem to be addressed. Second, parameterizations are constructed for spatial modulation of heat diffusion patterns that use path-weighted sums of analytical basis functions. Third, prototype analyses are presented for the purpose demonstrating various aspects of parameterizations that represent spatial modulation of heat diffusion patterns where there exist inhomogeneous or anisotropic thermal diffusivity. And finally, a conclusion is given.

S.G. Lambrakos and **K.P. Cooper**, Materials Science and Technology Division, Code 6390, Naval Research Laboratory, Washington, DC 20375-5320. Contact e-mails: lambrakos@nrl.navy.mil and lambrakos@anvil.nrl.navy.mil.

2. Definition of Inverse Heat Deposition Problem

In this section, a specific definition of the inverse heat deposition problem is presented. This presentation, which is redundant since it has been given within a number of previous studies, is necessary for establishing firmly the formal context of the inverse analysis methodology that is applied here.

The inverse problem concerning analysis of processes involving heat transfer (Ref 2-10), may be stated formally in terms of source functions (or input quantities) and multidimensional fields (output quantities). The statement of the inverse problem given in this article is focused on aspects of the inverse heat deposition problem related to the determination of heat

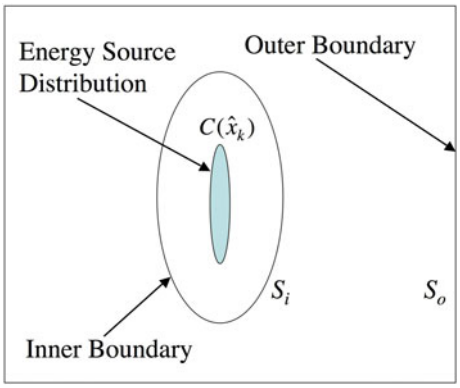

Fig. 1 Schematic representation of inner and outer boundaries of temperature field, which define inverse heat deposition problem, and weighting influences on temperature field associated with energy deposition

fluxes that can be extended to the modeling of heat diffusion in materials having inhomogeneous or anisotropic thermal diffusivity, i.e., a spatially dependent diffusivity function. This statement represents an extension of that given in Ref 11. In general, the formulation of a heat conducting system occupying an open bounded domain Ω with an outer boundary S_o and an inner boundary S_i (see Fig. 1) involves the parabolic equation

$$\frac{\partial T(\hat{x},t)}{\partial t} = \nabla \cdot (\kappa(\hat{x},t)\nabla T(\hat{x},t)) \qquad \text{(Eq 1a)}$$

for $T(\hat{x},t)$ in $\Omega \times (0,t_f)$, with initial condition $T(\hat{x},0) = T_0(\hat{x})$ in Ω, and heat flux exchanges through the outer and inner boundaries S_o and S_i as follows:

$$-\kappa(\hat{x},t)\frac{\partial T(\hat{x},t)}{\partial n_{S_o}} = c(\hat{x},t)(T(\hat{x},t) - T_a(\hat{x},t)) \qquad \text{(Eq 1b)}$$

on $S_o \times (0,\ t_f)$, and

$$-\kappa(\hat{x},t)\frac{\partial T(\hat{x},t)}{\partial n_{S_i}} = q(\hat{x},t) \qquad \text{(Eq 1c)}$$

on $S_o \times (0,\ t_f)$. Here $\hat{x} = (x,y,z)$ is the position vector, n_{S_o} and n_{S_i} are the normal vectors onto boundary S_o and S_i, respectively, t is the time variable, t_f is the final time, $T(\hat{x},t)$ is the temperature field variable, $\kappa(\hat{x},t)$ is the thermal diffusivity field variable, $c(\hat{x},t)$ and $T_a(\hat{x},t)$ are specified functions, and $q(\hat{x},t)$ is the heat flux on the inner boundary S_i. Determination of the temperature field via solution of Eq 1a-1c defines the direct initial-boundary value problem. The inverse problem considered here is that of effectively reconstructing the heat flux field $q(\hat{x},t)$ on the inner and outer boundaries S_i and S_o, and the resulting temperature field $T(\hat{x},t)$ for all time $t \in [0,t_f]$ when S_i and S_o are totally or partially inaccessible. In order to reconstruct the heat flux, information on the temperatures $T(\hat{x}_S,t)$, where $\{\hat{x}_S\} \in S_i, S_o$ is needed and, therefore, must be acquired either experimentally or via direct numerical simulation (Ref 12-22).

Following the gray-box inverse analysis approach, a parametric representation based on a physical model provides a means for the inclusion of information concerning the physical characteristics of a given energy deposition process. It follows then that for heat deposition processes involving the deposition of heat within a bounded region of finite volume, consistent parametric representations of the temperature field are given by

$$T(\hat{x},t,\kappa) = T_A + \sum_{k=1}^{N_k} T_k(\hat{x},\hat{x}_k,t,\kappa;\alpha_1,\ldots,\alpha_n) \quad \text{and}$$
$$T(\hat{x}_n^c,t_n^c,\kappa) = T_n^c \qquad \text{(Eq 2)}$$

where the quantity T_A is the ambient temperature of the workpiece and the locations $\hat{x}_n^c$ and temperature values T_n^c specify constraint conditions on the temperature field. The functions $T_k(\hat{x},\hat{x}_k,t,\kappa;\alpha_1,\ldots,\alpha_n)$ represent an optimal basis set of functions for given sets of boundary conditions and material properties. The quantities $\hat{x}_k = (x_k,y_k,z_k)$, $k = 1,\ldots,N_k$, are the locations of the elemental source or boundary elements. The sum defined by Eq 2 can for certain systems specify numerical integration over the discrete elements of a distribution of sources or boundary elements. Selection of an optimal set of basis functions is based on a consideration of the characteristic model and data spaces of heat deposition processes and subsequently isolating those regions of the model space corresponding to parameterizations that are both physically consistent and sufficiently general in terms of their mathematical representation and mapping from data to model space. Although heat deposition processes may be characterized by complex coupling between the heat source and workpiece, as well as complex geometries associated with either the workpiece or deposition process, in terms of inverse analysis the general functional forms of the temperature fields associated with all such processes are within a restricted class of functions, i.e., optimal sets of functions. Accordingly, a sufficiently optimal set of functions are analytic solutions to heat conduction equation for a finite set of boundary conditions (Ref 23). A parameterization based on this set is both sufficiently general and convenient relative to optimization.

The formal procedure underlying the inverse method considered here entails the adjustment of the temperature field defined over the entire spatial region of the sample volume at a given time t. This approach defines an optimization procedure where the temperature field spanning the spatial region of the sample volume is adopted as the quantity to be optimized. The constraint conditions are imposed on the temperature field spanning the bounded spatial domain of the workpiece by minimization of the value of the objective functions defined by

$$Z_T = \sum_{n=1}^{N} w_n\left(T(\hat{x}_n^c,t_n^c,\kappa) - T_n^c\right)^2 \qquad \text{(Eq 3)}$$

where T_n^c is the target temperature for position $\hat{x}_n^c = (x_n^c,y_n^c,z_n^c)$.

The input of information into the inverse model defined by Eq 1-3, i.e., the mapping from data to model space, is effected by: the assignment of individual constraint values to the quantities T_n^c; the form of the basis functions adopted for parametric representation; and specifying the shapes of the inner and outer boundaries, S_i and S_o, respectively, which bound the temperature field within a specified region of the workpiece. The constraint conditions and basis functions, i.e., $T(\hat{x}_n^c,t_n^c,\kappa) = T_n^c$ and $T_k(\hat{x},\hat{x}_k,\kappa,t;\alpha_1,\ldots,\alpha_n)$, respectively, provide for the inclusion of the following types of information: (a) solidification cross-sections (e.g., transverse, longitudinal, and top surface cross sections); (b) spatial character of energy source (e.g., position of maximum temperature, shape, and relative locations of vapor-liquid and liquid-solid boundaries); (c) geometric

information (e.g., shape features of workpiece and top surface of weld); (d) boundary conditions on workpiece; (e) information related to temperature history (e.g., microstructure correlation with temperature); (f) thermocouple measurements; (g) energy input (e.g., energy per distance); and (h) information based on physical model representations of aspects of heat deposition process, or results of numerical simulations.

Before proceeding, the following should be noted. First, the general trend features of heat deposition processes are such that the construction of a complete basis set of functions $T_k(\hat{x}, \hat{x}_k, t, \kappa; \alpha_1, \ldots, \alpha_n)$ making up a linear combination of the form defined by Eq 2 for representation of the associated temperature field is well defined and readily achievable. Second, for heat deposition processes, characteristics of the temperature field are poorly correlated to characteristics of the energy source. In contrast, however, the characteristics of the temperature field associated with these processes are strongly coupled to inner boundaries on this field, e.g., the solidification boundary. This property follows from the low-pass spatial filtering property of the basis functions $T_k(\hat{x}, \hat{x}_k, t, \kappa; \alpha_1, \ldots, \alpha_n)$, whose general forms are consistent with the dominant trend features of heat deposition processes. Third, given a consistent set of basis functions, the temperature field associated with a heat deposition process is completely specified by: the shape and temperature distribution of a given inner boundary on the domain of the temperature field; the diffusivity κ and speed of deposition V; and spatial dimensions, e.g., thickness D, of the workpiece. Fourth, the shape and temperature distribution of a specified inner boundary S_i is determined by the rate of energy deposited on the surface of the workpiece and the strength of coupling of the energy source to the workpiece. Finally, since an inner boundary S_i (see Fig. 1) is defined by its shape and the distribution of temperatures on its surface $T(\hat{x}_S)$, it follows that one can define a multidimensional temperature field $T(\hat{x}, \kappa, V, D, T(\hat{x}_S), \hat{x}_S \in S_i)$.

The existence of a convenient and general parameterization of inner boundary surfaces, $T(\hat{x}_S)$, $\hat{x}_S \in S_i$, bounding the temperature fields associated with heat deposition processes can be associated with the fact that all heat deposition processes are characterized by thermal and energy deposition profiles whose general form can be represented by a small class of geometric shapes. Accordingly, the observed volumetric distributions of energy from all types of heat deposition processes, within the inner boundary S_i of their associated temperature fields, can be represented by linear combinations of the basis functions that are within the class of generalized functions that are defined by the dominant trend features associated with volumetric energy deposition. These generalized functions provide for the construction of a relatively optimal and general parametric representation $T(\hat{x}, \kappa, V, D, T_s(\hat{x}_S), \hat{x}_S \in S_i, S_o)$ for inverse analysis of heat deposition processes. In doing so, referring to Fig. 1, the inverse problem defined by the mapping

$$C(\hat{x}_k) \mapsto T(\hat{x}) \qquad \text{(Eq 4)}$$

is replaced by the inverse problem defined by the mapping

$$C(\hat{x}_k), \kappa \mapsto S_i, S_o \mapsto T(\hat{x}). \qquad \text{(Eq 5)}$$

Following the same arguments, the definition of the inverse heat deposition problem as given above can be extended to include systems that are characterized by incomplete information concerning the diffusivity function κ. This would include any nonlinear dependence of κ on temperature, or in general, position in space. In addition, it is significant to note that Eq 5 establishes a foundation for the specification of weighted space-averaged disfussivities, and thus a foundation for parameterizations based on path-weighted diffussivity functions.

Relatively interesting sensitivity issues are observed to follow from inverse analysis defined according to the sequence of mappings Eq 5. The mathematical properties underlying these sensitivity issues are the same as those responsible for the ill disposition of many inverse analysis procedures based on the mapping Eq 4. That is to say, those filter properties of diffusion processes that tend to make the temperature field $T(\hat{x})$ insensitive to details of the shape of the source distribution $C(\hat{x}_k)$, tend to make $T(\hat{x})$ insensitive to localized spatial variations in the shapes of S_i and S_o. This insensitivity to details of the shapes of S_i and S_o, e.g., localized spatial variations in the shape of the solidification boundary, implies that parametric representations of the inner and outer boundaries, S_i and S_o, can be formulated in terms of relatively convenient mathematical forms.

3. Parameterizations Using Analytical Basis Functions and Path-Weighted Diffusivity Functions

As demonstrated in previous studies, many energy deposition processes are characterized by volumetric coupling of the energy source and associated heat diffusion patterns that are relatively complex. Accordingly, it is advantageous to extend the adjustability of the general parameterization defined by Eq 2 for the purpose of representing more complex diffusion patterns. As shown previously, the adjustability of the parameterization can be extended by adopting basis functions whose spatial distributions are spatially modulated. Among the many different possible types of spatial modulation that can be applied are those whose application produces diffusion patterns that are directionally or path weighted. The extension of the parameterization defined by Eq 2 for the inclusion of spatial modulation can be expressed by

$$\begin{aligned} &T(\hat{x}, t, \kappa, V, D, T_s(\hat{x}_S), \hat{x}_S \in S_i, S_o) \\ &\quad = T(\hat{x}, t, \kappa_m(\hat{x}), C(\hat{x}_k), \hat{x}_k, t_k, \Delta t, N_t, N_k, V_k). \end{aligned} \qquad \text{(Eq 6)}$$

Given the parameterization framework defined by Eq 6, it follows that the consistent representations of the temperature field in terms of basis functions and path-weighted diffussivity functions, which can be associated with anisotropic or directionally dependent heat diffusion, are

$$T(\hat{x}, t) = T_A + \sum_{k=1}^{N_k} \sum_{n=1}^{N_t} C(\hat{x}_k) F(\hat{x}, \hat{x}_k, n\Delta t, \kappa_m(\hat{x})) \delta(n\Delta t - t_k) \qquad \text{(Eq 7)}$$

where

$$\begin{aligned} &F(\hat{x}, \hat{x}_k, t, \kappa_m(\hat{x})) \\ &\quad = \frac{1}{t} \exp\left[-\frac{(x - x_k)^2 + (y - y_k)^2}{4\kappa_m(\hat{x}) t} \right] \\ &\qquad \times \left\{ 1 + 2 \sum_{m=1}^{\infty} \exp\left[-\frac{\kappa_m(\hat{x}) m^2 \pi^2 t}{l^2} \right] \cos\left[\frac{m\pi z}{l} \right] \cos\left[\frac{m\pi z_k}{l} \right] \right\}, \end{aligned} \qquad \text{(Eq 8)}$$

$t = N_t \Delta t$ and $\delta(t)$ is the Dirac delta function representing the instantaneous deposition at locations $\hat{x}_k = (x_k, y_k, z_k)$ at times $t = t_k$. The speed of energy deposition V_k, which is an implicit function of position on the surface of the workpiece, is given by

$$V_k = \frac{x_k - x_{k-1}}{t_k - t_{k-1}}. \quad \text{(Eq 9)}$$

Another consistent representation of the temperature field in terms of basis functions and path-weighted diffusivity is

$$T(\hat{x}, t) = T_A + \sum_{k=1}^{N_k} \sum_{n=1}^{N_t} C(\hat{x}_k) G(\hat{x}, \hat{x}_k, n\Delta t, V_k, \kappa_m(\hat{x})) \quad \text{(Eq 10)}$$

where

$$G(\hat{x}, \hat{x}_k, t, V_k, \kappa_m(\hat{x})) = \frac{1}{t} \exp\left[-\frac{(x - x_k - V_k t)^2 + (y - y_k)^2}{4\kappa_m(\hat{x}) t}\right] \times \left\{1 + 2\sum_{m=1}^{\infty} \exp\left[-\frac{\kappa_m(\hat{x}) m^2 \pi^2 t}{l^2}\right] \cos\left[\frac{m\pi z}{l}\right] \cos\left[\frac{m\pi z_k}{l}\right]\right\} \quad \text{(Eq 11)}$$

and

$$C(x, y, z) = \sum_{k=1}^{N_k} q(x, y, z_k) \delta(z - z_k), \quad \text{(Eq 12)}$$

where $\delta(z)$ is the Dirac delta function, and $\{q(x, y, z_k), z_k\}$, $k = 1,\ldots,N_k$, represent adjustable parameters. Referring to Eq 7 through 12, it is to be noted that spatial modulation of the diffusion field is through functional dependence on the generalized diffusivity function $\kappa_m(\hat{x})$ and the adjustable parameters Δt, N_t, N_k, and V_k. Consistent with the generalized mapping represented by Eq 6, the parameter V_k, which can be a function of the discrete index k, can assume values that are in general not equal to the speed of the energy source V relative to the workpiece. Accordingly, the procedure for inverse analysis defined by Eq 7-12 entails adjustment of the parameters $C(\hat{x}_k)$, $\hat{x}_k$, Δt and V_k defined over the entire spatial region of the workpiece.

At this stage, it is appropriate to establish interpretation of the parameterizations expressed by the basis functions defined by Eq 7 through 12. First, it must be emphasized that the primary set of parameters for system representation, which are uniquely defined, are the quantities $(V, D, \kappa, T_s(\hat{x}_S),\ \hat{x}_S \in S_i, S_o)$, although it is assumed *a priori* that information concerning these quantities may be incomplete or not available. Second, the weighted sums of basis functions defined by Eq 7 through 12 establish a set of parameters, which are not uniquely defined, but establish the mapping expressed by Eq 6. Accordingly, the mapping from one set of parameters to another, defined by Eq 6, provides a general framework for a more general and flexible parameterization of the temperature field $T(\hat{x}, t, V, D, \kappa, T_s(\hat{x}_S),\ \hat{x}_S \in S_i, S_o)$. The necessity of a more general and flexible parameterization follows from the specific definition of the inverse heat transfer problem that is being considered, and the associated conditions for its application. That is to say, the goal of any inverse analysis following the general procedure being considered is construction of a temperature field $T(\hat{x}, t, \kappa, V, D, T_s(\hat{x}_S),\ \hat{x}_S \in S_i, S_o)$ where the surface distribution of temperatures $T_s(\hat{x}_S)$, $\hat{x}_S \in S_i, S_o$, represents the only constraint condition on the calculated temperature field. Accordingly, parameterizations that are sufficiently flexible and convenient with respect to variation of heat diffusion patterns are required.

In its simplest form $\kappa_m(\hat{x}) = \kappa_0$, a constant value approximately equal to the average diffusivity κ of the material of the workpiece. In its most general form, $\kappa_m(\hat{x})$ is a relatively complex function that varies nonlinearly with $\hat{x}$. For specific cases, $\kappa_m(\hat{x})$ can be generalized to represent a spatially weighted average diffusivity using the expression

$$\kappa_m(x) = (1 - x/L)\kappa_1 + (x/L)\kappa_2 \quad \text{(Eq 13)}$$

where κ_1, κ_2, and L can in principle be phenomenological adjustable parameters or quantities related to actual material diffusivities and workpiece dimensions. A two-dimensional (2D) extension of Eq 13 is given by

$$\kappa_m(x, y) = \left(1 - \sqrt{x^2 + y^2}/L\right)\kappa_1 + \left(\sqrt{x^2 + y^2}/L\right)\kappa_2 \quad \text{(Eq 14)}$$

Next, given that a function $\kappa_m(\hat{x})$ has been specified, one type of path-weighted average diffusivity can be given by

$$\langle \kappa_m(r, \theta) \rangle = \frac{1}{r} \int_0^r \kappa(r', \theta) dr' = \frac{1}{r} \sum_{k=1}^{N_k} \kappa(k\Delta r, \theta)\Delta r = \frac{1}{N_k} \sum_{k=1}^{N_k} \kappa(k\Delta r, \theta). \quad \text{(Eq 15)}$$

The functionality expressed by Eq 15 provides a directional path-integral weighting of the heat diffusion pattern. This directional path-weighting, however, defines a path-integral near-neighbor's problem that is associated with the directional tracking of diffusivity values along any given path. It follows that approximations of the path integral defined by Eq 15 would provide for more computational efficiency. An approximation of Eq 15 is given by

$$\langle \kappa_m(r, \theta) \rangle = \frac{1}{r} \int_0^r \kappa(r', \theta) dr' \approx \frac{1}{2}[\kappa(\Delta r, \theta) + \kappa(N_k \Delta r, \theta)]. \quad \text{(Eq 16)}$$

At this point it is significant to note that the weighted averages defined by Eq 13 through 16 provide a spatial modulation of the temperature field that is essentially phenomenological in nature. That is to say, although modulation of the temperature field using Eq 13-16 is consistent with the general trend features of path-weighted diffusivities, the average diffusivity functions given by Eq 13-16 are not defined with respect to a path-weighted average that is consistent with the form of Eq 8 and 11. Accordingly, a path-weighted average diffusivity can be derived with respect to the formal structures of Eq 8 and 11. The formal structures of Eq 8 and 11 imply that a more physically consistent path-weighted average is with respect to the inverse of the diffusivity function, i.e., $1/\kappa$, and therefore that a quantity $\langle \kappa_m \rangle$ can be defined by the expression

$$\frac{1}{\langle \kappa_m(r, \theta) \rangle} = \frac{1}{r} \int_0^r \frac{dr'}{\kappa(r', \theta)} \approx \frac{1}{2}\left[\frac{1}{\kappa(\Delta r, \theta)} + \frac{1}{\kappa(N_k \Delta r, \theta)}\right] = \frac{\kappa(\Delta r, \theta) + \kappa(N_k \Delta r, \theta)}{2\kappa(\Delta r, \theta)\kappa(N_k \Delta r, \theta)}. \quad \text{(Eq 17)}$$

Next, given that the origins of the discrete paths are associated with the discrete source distribution $C(\hat{x}_k)$, it follows from Eq 17 that

$$\langle \kappa_m(\hat{x}_k, \hat{x}) \rangle = \frac{2\kappa(\hat{x}_k)\kappa(\hat{x})}{\kappa(\hat{x}_k) + \kappa(\hat{x})}. \quad \text{(Eq 18)}$$

Since the directional path-weighting defined by Eq 18 represents a path-integral mean value, directional tracking of diffusivity values at near neighbor locations is not required.

4. Prototype Analysis I

In this section, prototype calculations that consider energy deposition within a material characterized by inhomogeneous and anisotropic thermal diffusivity are presented. These calculations demonstrate application of the general algorithmic structure presented above to the inverse analysis of energy deposition processes where there exists inhomogeneous and anisotropic thermal diffusivity. The prototype system is that of freeform fabrication of a 2D coupon for a system whose thermal diffusivity is a function of position. The model system consists of a sequence of layers, where each layer consists of a distribution of discrete energy sources whose strengths are assigned by the values of the coefficients $C(\hat{x}_k, n\Delta t)$ defined in Eq 7 and are numerically integrated at each time step. Each of the discrete energy sources represents a discrete liquid metal droplet of a given volume. The translation speed of the fabricated coupon relative to the points of liquid metal deposition is assigned implicitly through the time dependence and relative locations of the discrete energy sources, $C(\hat{x}_k, n\Delta t)$. That is to say, a certain number of drops per layer and a certain number of layers as a function of time are specified. The model parameters used for the prototype analysis are listed in Table 1. For purposes of this analysis, the basis function $F(\hat{x}, \hat{x}_k, t, \kappa)$ given by Eq 8 is adopted for calculation of the temperature field. These functions are the solutions to the heat conduction equations for temperature-independent diffusivity and non-conducting boundaries on two surfaces that are separated by a distance l, which will correspond to the thickness of the coupon to be fabricated. Accordingly, it is assumed for this simulation that there is no conduction at the substrate boundary. An additional condition imposed on the model system is that of heat transfer into the ambient environment at the edges of the 2D coupon being fabricated. This is a realistic assumption for process conditions where droplet-by-droplet deposition occurs within a mold structure consisting of a metal powder composite thermal diffusivity of which is similar to that of the fabricated structure, e.g., rectangular coupon. A constraint condition imposed on the temperature field is that the liquid-solid interface defined by the alloy liquidus temperature is at that of the specific alloy at any given position within the material. Accordingly, the values assigned to the coefficients $C(\hat{x}_k, n\Delta t)$ were such that the average temperature of each discrete droplet was within the range of liquid metal. It is significant to note that other constraint conditions such as melt-pool dimensions and measurements of temperature via thermocouples can also be adopted for assigning values to the coefficients $C(\hat{x}_k, n\Delta t)$. In the prototype analysis under study, the layers are deposited one on top of the other by traversing the passes in a zig-zag fashion. Consistent with the filter properties associated with thermal diffusion, each liquid-metal droplet can be represented by a cube, or rectangle in two-dimensions (see Table 1). This follows from the spatial filtering property of the dominant trend factor that is given by Eq 8, which implies that the temperature field is insensitive to details of the shape of the liquid-metal droplet. It is significant to note, however, that the temperature field does have sensitivity with respect to the spatial distribution of droplets. This sensitivity is demonstrated by the calculations presented later. The prototype analysis considers calculation of the temperature field at a sampling point within the model structure.

Table 1 Model parameters used to determine thermal fields in droplet-by-droplet deposition process

Model parameters
Material: Cu-Ni alloy distribution
Diffusivity: Given by Eq 13
Timestep: $\Delta t = 0.005$ s
Drop deposited every 5 timesteps
11 drops per layer
Droplet energy content: $C(\hat{x}_k, n\Delta t) = 4.0$
Droplet volume = $(\Delta l)^3$, $\Delta l = 0.1667$ cm

The prototype analysis is characterized by energy deposition within a material having inhomogeneous and anisotropic thermal diffusivity. The system, which consists of a 2D discrete distribution of Cu-Ni alloys of variable relative percentage as a function of position, is described schematically in Fig. 2. This alloy distribution is characteristic of that which would be constructed by drop-by-drop liquid metal deposition of 11 alloys (differing in wt.%) being dropped sequentially to build-up a thin wall. For this system, the liquidus temperature is also a function of relative alloy composition. A diffusivity function and average liquidus temperature field are constructed according to the 2D discrete distribution of Cu-Ni alloys. Accordingly,

$$\kappa_m(x,y,z) = (1 - x/L)\kappa_1 + (x/L)\kappa_2 \text{ and}$$
$$T_M(x,y,z) = (1 - x/L)T_{M1} + (x/L)T_{M2} \quad \text{(Eq 19)}$$

where $\kappa_1 = 1.136 \times 10^{-4}$ m^2/s, and $T_{M1} = 1085$ °C, corresponding to pure Copper, and $\kappa_2 = 2.303 \times 10^{-4}$ m^2/s and $T_{M2} = 1455$ °C, corresponding to pure Nickel. The prototype analysis that follows consists of temperature field calculations that demonstrate the influence of path-weighted diffusivity on heat diffusion patterns according to adjustment of the various

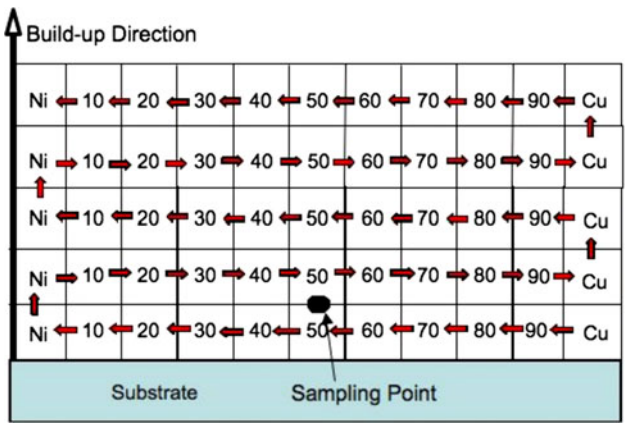

Fig. 2 Schematic representation of drop-by-drop liquid metal-deposition process assumed for construction of a five-layer structure

parameters associated with the basis functions defined by Eq 7 through 9. We consider the calculations of temperature fields that adopt the spatially dependent diffussivity function Eq 19, the constant diffusivities $\kappa_1 = 1.136 \times 10^{-4}$ m^2/s and $\kappa_2 = 2.303 \times 10^{-4}$ m^2/s, corresponding to pure Copper and Nickel, respectively, and adjusted discrete spatial distributions of the effective heat source given by Eq 7, so that the calculated cross sections of the solidification boundary satisfy, in principle, experimentally observed solidification patterns or droplets of given volume whose average temperature, which is above that of liquidus, has been specified. The results of these calculations are shown in Fig. 3 for the weighted sums of basis functions defined by Eq 7.

Shown in Fig. 3(a)-(e) are the time-dependent temperature fields at different stages of the droplet-by-droplet liquid metal deposition processes during the formation of a structure consisting of five layers according to the sequence defined by Fig. 2. Referring to these figures, one can establish a visual correlation of the temperature history at any given sampling point with the relative position of the liquid metal droplet at time of deposition. Accordingly, the temperature history at the sample point indicated in Fig. 2 can be examined relative to the position of the liquid metal droplet of the Cu-Ni alloy composite at all stages of the droplet sequence, as well as, relative to the temperature fields corresponding to pure Cu and Ni. The results of this type of calculation are shown in Fig. 4.

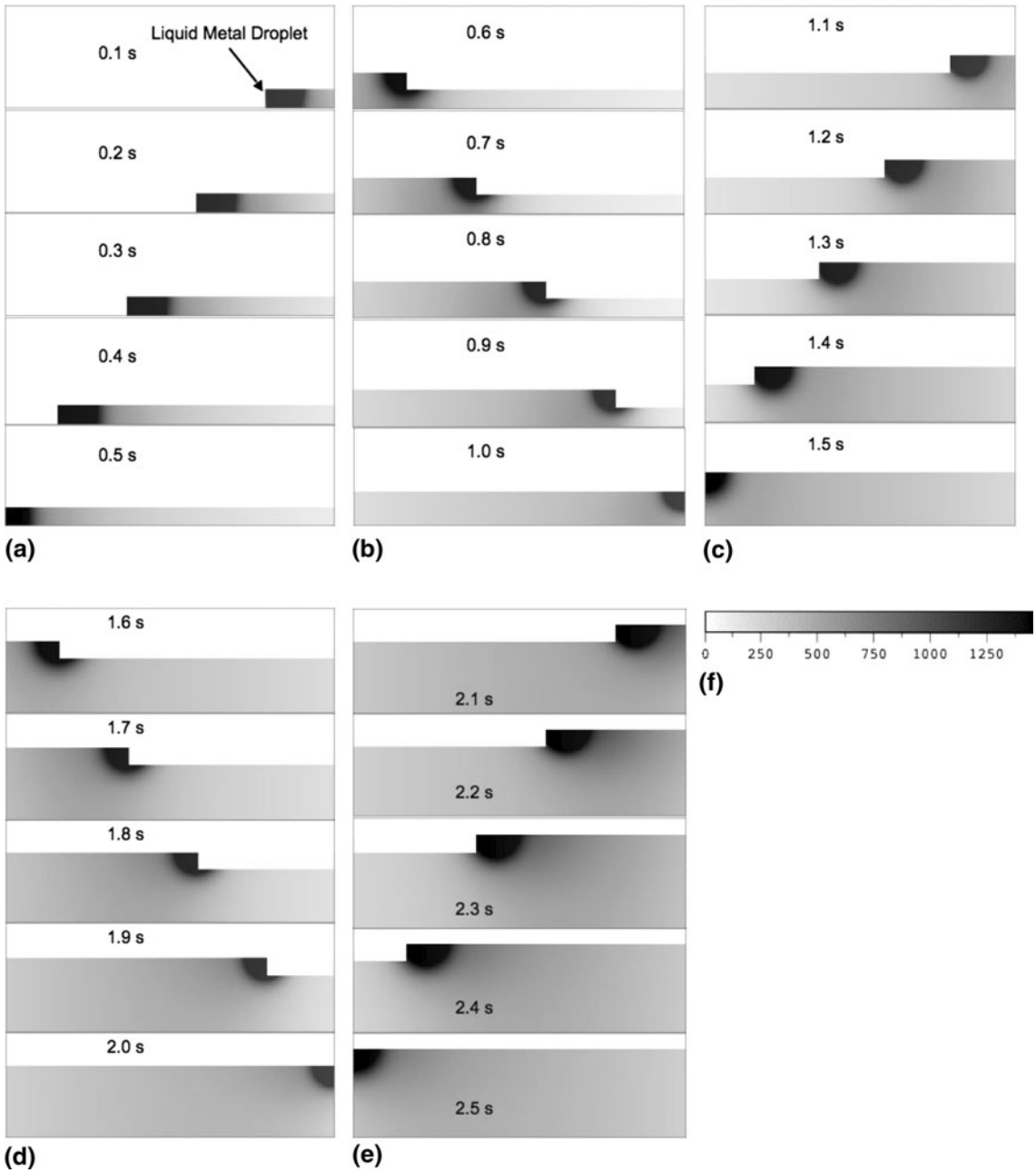

Fig. 3 Two-dimensional temperature field (°C) of built structure during formation of (a) first layer, (b) second layer, (c) third layer, (d) fourth layer, and (e) fifth layer, each consisting of Cu-Ni alloy composite. (f) Temperature field gray scale from 0 to 1455 °C for (a)-(e)

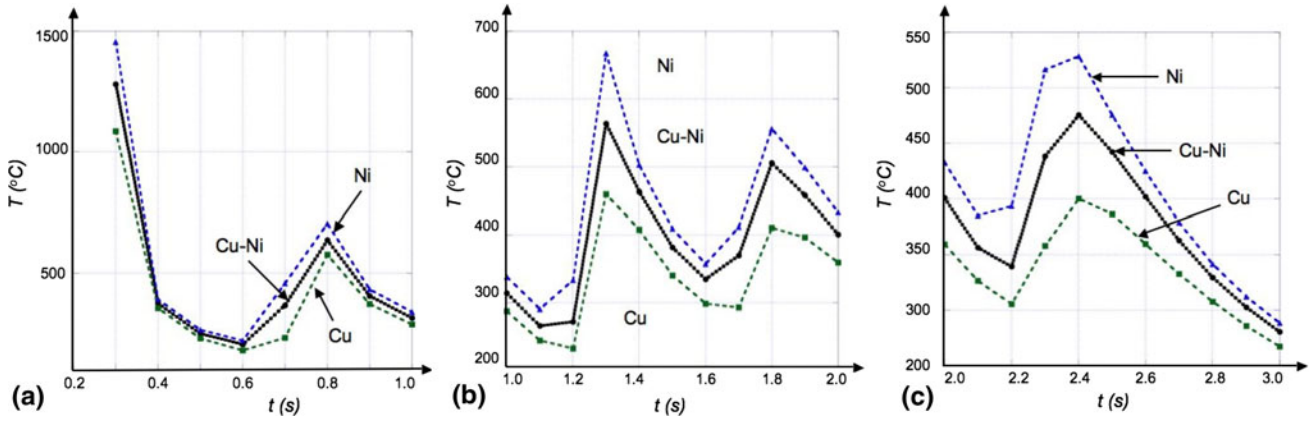

Fig. 4 Temperature histories at sample point shown in Fig. 2 within built structures consisting of Pure Cu, Pure Ni and Cu-Ni alloy composite for time period (a) 0.2-1.0 s, (b) 1.0-2.0 s, and (c) 2.0-3.0 s

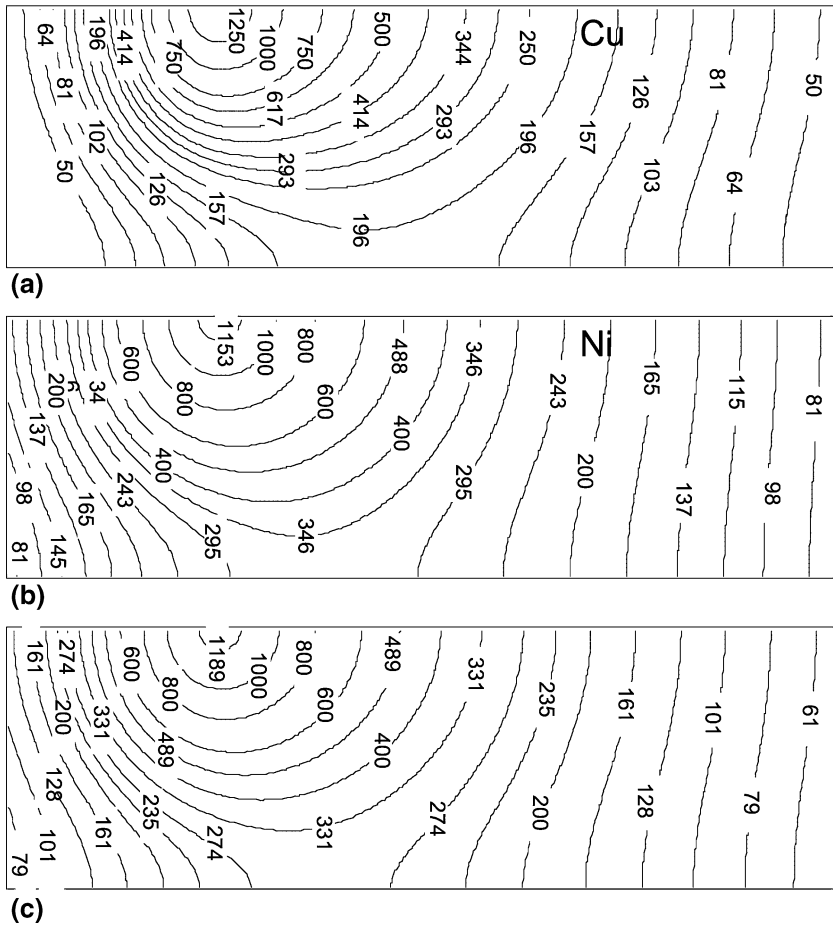

Fig. 5 Slices of three-dimensional temperature fields (°C) at symmetry plane calculated using basis functions defined by Eq 10 through 12. Temperature fields corresponding to diffusivity for (a) Pure Cu, (b) Pure Ni; and (c) Temperature field corresponding to phenomenological diffusivity function $\kappa_m(\hat{x})$ defined by Eq 13, where relative motion of heat source is in direction of monotonic increase of $\kappa_m(\hat{x})$

4.1 Discussion

At this point, the calculations shown in Fig. 3 and 4 are examined with respect to the inverse analysis formalism defined above. Referring to these figures, one can associate the boundary defined by the liquidus temperature (see Fig. 3) with an inner boundary S_i, and similarly, the temperature history shown in Fig. 4 with a point on the surface of an outer boundary S_o. It is to be noted then, that in principle, temperatures associated with both S_i and S_o are experimentally observable and, therefore, adoptable as constraints for application of the procedure defined Eq 2 and 3.

An interesting qualitative result of the calculations shown in Fig. 4 is that they demonstrate reasonable sensitivity of temperature histories to alloy distribution within a material. This implies that alloy distribution can, in principle be adopted as a process parameter for control of temperature history, as well as, droplet size and energy content. Control of temperature history would imply, in turn control of microstructure within structure that is built by means of drop-by-drop metal depsoition.

5. Prototype Analysis II

In this section, prototype calculations that demonstrate the use of spatially dependent diffusivity functions for spatial modulation of the heat diffusion pattern with respect to specified constraint conditions are presented. Therefore, it follows that for the parameterization defined by Eq 8, spatial dependence of the diffusivity function is not to be associated with an actual inhomogeneous or anisotropic thermal diffusivity of the material, but rather with a phenomenological weighting of the steady-state diffusion pattern for an energy source moving relative to the workpiece. It is significant to indicate again that the necessity of more general and flexible parameterizations of the temperature field follows from the specific definition of the inverse heat transfer problem that is being considered, and the associated conditions for its application. The use of a spatially dependent diffusivity function for purposes of weighting the steady-state diffusion pattern provides yet another flexible parameterization of the temperature field for its convenient adjustment with respect to constraint conditions. In other words, a spatially dependent diffusivity function extends adjustability of the temperature field for the mapping defined by Eq 6 according to the generalization of Eq 5 given by

$$C(\hat{x}_k), \kappa(\hat{x}) \mapsto S_i, S_o \mapsto T(\hat{x}) \qquad \text{(Eq 20)}$$

For the parameterization defined by Eq 10-12, the temperature field was calculated using the parameter values $\Delta t = 6.0 \times 10^{-3}$ s, $N_t = 40$, $l = 1$ cm, $V_k = 0.06$ m/s, and $\{q(z_0), \ldots q(z_4)\} = \{0.45, 0.36, 0.18, 0.18, 0.18\}$, where $z_k = 0.833k$ mm, with $k = 0, \ldots, 4$. The results of these calculations are shown in Fig. 5 and 6. The purpose of these calculations is to demonstrate some general functional characteristics associated with the adjustment of the steady-state temperature field by means of a spatially dependent phenomenological diffusivity function. Shown in Fig. 5 and 6 are

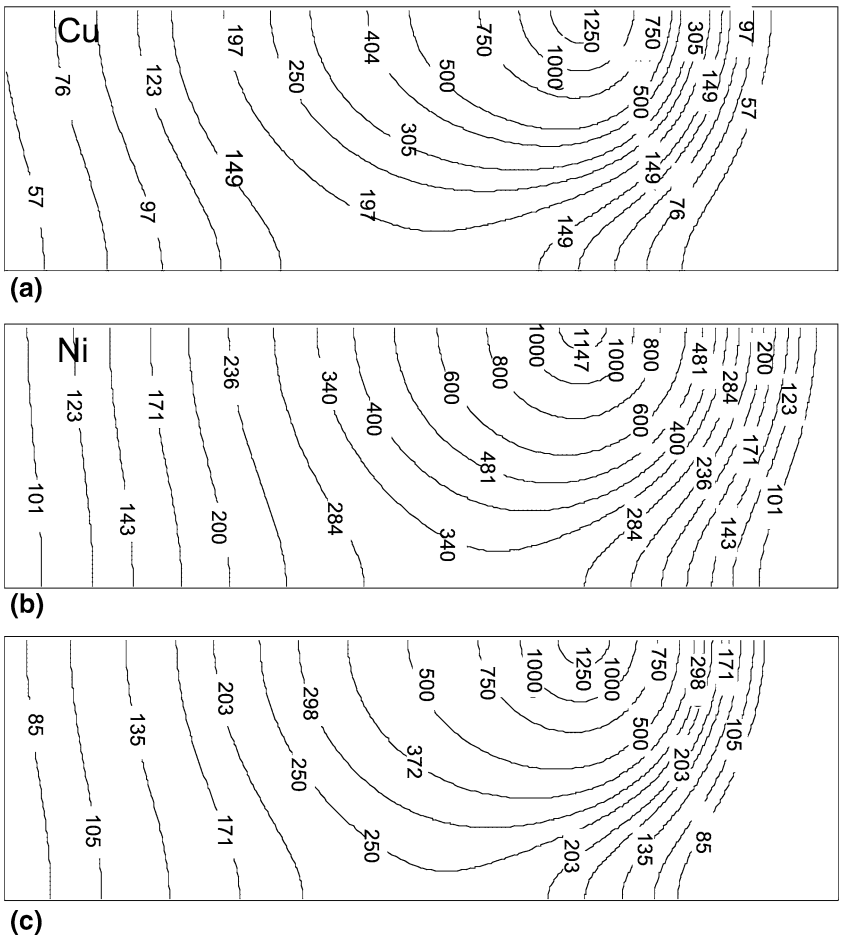

Fig. 6 Slices of three-dimensional temperature fields (°C) at symmetry plane calculated using basis functions defined by Eq 10 through 12. (a) Temperature fields corresponding to diffusivity for (a) Pure Cu, (b) Pure Ni; and (c) Temperature field corresponding to phenomenological diffusivity function $\kappa_m(\hat{x})$ defined by Eq 13, where relative motion of heat source is in direction of monotonic decrease of $\kappa_m(\hat{x})$

steady-state temperature fields corresponding to energy deposition within the volume of a workpiece consisting of pure Cu, pure Ni, and an arbitrary material whose temperature field is to be determined by inverse analysis according to observed constraint conditions. Referring to both figures, comparison of the diffusivity function-modulated temperature fields, Fig. 5(c) and 6(c), to those calculated for constant diffusivities demonstrates the general functional characteristics of using a spatially dependent diffusivity function for modulation of the steady-state heat diffusion pattern.

5.1 Discussion

At this point, the calculations shown in Fig. 5 and 6 are examined with respect their correlation with physically consistent trends that would in principle be inverse analyzed. Shown in Fig. 5(c) and 6(c) are temperature fields calculated using the phenomenological diffusivity function $\kappa_m(\hat{x})$ defined by Eq 13, where relative motion of heat source is in direction of monotonic increase and decrease, respectively, of the value of the function $\kappa_m(\hat{x})$. Referring to these figures, it is significant to note that the modulation of heat diffusion that is induced by means of $\kappa_m(\hat{x})$ is physically consistent with influences on energy-workpiece coupling, where coupling of the energy transport to fluid convection exists.

6. Conclusion

The objective of this article was to present a preliminary description of general parameterizations of time-dependent temperature fields occurring in heat deposition processes where inhomogeneous or anisotropic thermal diffusivity exists. These parameterizations are in terms of basis functions and path-weighted diffusivity functions and follow from a specific and restricted definition of the inverse heat transfer problem. This definition of the inverse heat transfer problem, which establishes a well-disposed definition of the inverse heat deposition problem, permits both convenience and flexibility with respect to process parameterization for purposes of inverse analysis. Prototype analyses that demonstrate the application of the general algorithmic structure for inverse analysis of materials having spatially dependent thermal diffusivity were presented. Further analyses are required to examine sensitivity issues related to the application of different average representations of path-weighted diffusivity functions, i.e., Eq 13 through 18, as well as, further application of the basis function formalism defined by Eq 7 through 12 to inverse analysis of different types of energy deposition processes where thermal diffusivity is strongly dependent upon position.

Acknowledgment

The authors thank the Office of Naval Research for its support in performing this research.

References

1. A. Tarantola, *Inverse Problem Theory and Methods for Model Parameter Estimation*, SIAM, Philadelphia, PA, 2005
2. M.N. Ozisik and H.R.B. Orlande, *Inverse Heat Transfer, Fundamentals and Applications*, Taylor and Francis, New York, 2000
3. K. Kurpisz and A.J. Nowak, *Inverse Thermal Problems*, Computational Mechanics Publications, Boston, USA, 1995
4. O.M. Alifanov, *Inverse Heat Transfer Problems*, Springer, Berlin, 1994
5. J.V. Beck, B. Blackwell, and C.R. St. Clair, *Inverse Heat Conduction: Ill-Posed Problems*, Wiley Interscience, New York, 1985
6. J.V. Beck, Inverse Problems in Heat Transfer with Application to Solidification and Welding, *Modeling of Casting, Welding and Advanced Solidification Processes V*, M. Rappaz, M.R. Ozgu, and K.W. Mahin, Ed., The Minerals, Metals and Materials Society, 1991, p 427–437
7. J.V. Beck, Inverse Problems in Heat Transfer, *Mathematics of Heat Transfer*, G.E. Tupholme and A.S. Wood, Ed., Clarendon Press, 1998, p 13–24
8. N. Zabaras, Inverse Modeling of Solidification and Welding Processes, *Modeling of Casting, Welding and Advanced Solidification Processes*, V.M. Rappaz, M.R. Ozgu, and K.W. Mahin, Ed., The Minerals, Metals and Materials Society, 1991, p 523–530
9. G.S. Dulikravich and T.J. Martin, Inverse Shape and Boundary Condition Problems and Optimization, *Heat Conduction: Advances in Numerical Heat Transfer*, Vol 1, Chapter 10, W.J. Minkowycz and E.M. Sparrow, Ed., Taylor & Francis, 1996, p 381–426
10. T.J. Martin and G.S. Dulikravich, Inverse Determination of Boundary Conditions in Steady Heat Conduction with Heat Generation, *ASME J. Heat Transfer*, 1996, **118**, p 546–554
11. J. Xie and J. Zou, Numerical Reconstruction of Heat Fluxes, *SIAM J. Numer. Anal.*, 2005, **43**(4), p 1504–1535
12. S.G. Lambrakos and J.G. Michopoulos, Algorithms for Inverse Analysis of Heat Deposition Processes, *Mathematical Modelling of Weld Phenomena*, Vol 8, Verlag der Technischen Universite Graz, Austria, 2007, p 847
13. S.G. Lambrakos and J.G. Michopoulos, Computational Parameterization Simplicity and Filtering of Data-Driven Inverse Analysis for Heat Deposition Processes, *Proceedings of IDETC/CIE 2006, ASME 2006 International Design Engineering Technical Conferences & Computers and Information in Engineering Conference*, September 10-13, 2006, Philadelphia, Pennsylvania, USA
14. S.G. Lambrakos and J.O. Milewski, Analysis of Welding and Heat Deposition Processes using an Inverse-Problem Approach, *Mathematical Modelling of Weld Phenomena*, Vol 7, Verlag der Technischen Universite Graz, Austria, 2005, p 1025–1055
15. P.G. Moore, H.N. Jones, III, and S.G. Lambrakos, An Inverse Heat Transfer Model of Thermal Degradation Within Multifunctional Tensioned Cable Structures, *J. Mater. Eng. Perform.*, 2005, **14**(1), p 112–118
16. S.G. Lambrakos and J.O. Milewski, Analysis of Processes Involving Heat Deposition Using Constrained Optimization, *Sci. Technol. Weld. Join.*, 2002, **7**(3), p 137
17. S.G. Lambrakos and D.W. Moon, Analysis of Welds Using Geometric Constraints, *Computer-Aided Design, Engineering, and Manufacturing, Systems Techniques and Applications*, C. Leondes, Ed., CRC Press, New York, 2001
18. S.G. Lambrakos, E.A. Metzbower, J.O. Milewski, G. Lewis, R. Dixon, and D. Korzekwa, Simulation of Deep Penetration Welding Processes Using Geometric Constraints Based on Experimental Information, *J. Mater. Eng. Perform.*, 1994, **3**(5), p 639
19. K.P. Cooper and S.G. Lambrakos, Fabrication of Net-Shaped Metallic Parts by Overlapping Reinforcement Weld Beads, *Proceedings of the Seventh International Conference on Trends in Welding Research*, May 16-20, 2005 (Pine Mountain, Georgia), ASM International, Materials Park, Ohio, 2005, p 647
20. E.A. Metzbower, D.W. Moon, C.R. Feng, S.G. Lambrakos, and R.J. Wong, Modelling of HSLA-65 GMAW Welds, *Mathematical Modelling of Weld Phenomena*, Vol 7, Verlag der Technischen Universite Graz, Austria, 2005, p 327–339
21. S.G. Lambrakos, R.W. Fonda, J.O. Milewski, and J.E. Mitchell, Analysis of Friction Stir Welds Using Thermocouple Measurements, *Sci. Technol. Weld. Join.*, 2003, **8**, p 345
22. R.W. Fonda and S.G. Lambrakos, Analysis of Friction Stir Welds Using an Inverse Problem Approach, *Sci. Technol. Weld. Join.*, 2002, **7**(3), p 177
23. H.S. Carslaw and J.C. Jaegar, *Conduction of Heat in Solids*, 2nd ed., Clarendon Press, Oxford, 1959, p 374